Chapter 10

MRI Mapping of the Blood Oxygenation Sensitive Parameter T_2* in the Kidney: Basic Concept

Lu-Ping Li, Bradley Hack, Erdmann Seeliger, and Pottumarthi V. Prasad

Abstract

The role of hypoxia in renal disease and injury has long been suggested but much work still remains, especially as it relates to human translation. Invasive pO_2 probes are feasible in animal models but not for human use. In addition, they only provide localized measurements. Histological methods can identify hypoxic tissue and provide a spatial distribution, but are invasive and allow only one-time point. Blood oxygenation level dependent (BOLD) MRI is a noninvasive method that can monitor relative oxygen availability across the kidney. It is based on the inherent differences in magnetic properties of oxygenated vs. deoxygenated hemoglobin. Presence of deoxyhemoglobin enhances the spin–spin relaxation rate measured using a gradient echo sequence, known as R_2* (= $1/T_2$*). While the key interest of BOLD MRI is in the application to humans, use in preclinical models is necessary primarily to validate the measurement against invasive methods, to better understand physiology and pathophysiology, and to evaluate novel interventions. Application of MRI acquisitions in preclinical settings involves several challenges both in terms of logistics and data acquisition. This section will introduce the concept of BOLD MRI and provide some illustrative applications. The following sections will discuss the technical issues associated with data acquisition and analysis.

This chapter is based upon work from the COST Action PARENCHIMA, a community-driven network funded by the European Cooperation in Science and Technology (COST) program of the European Union, which aims to improve the reproducibility and standardization of renal MRI biomarkers. This introduction chapter is complemented by two separate chapters describing the experimental procedure and data analysis.

Key words Magnetic resonance imaging (MRI), Kidney, Mice, Rats, Blood oxygenation level dependent (BOLD) MRI, Hypoxia

1 Introduction

All organs exist in a state of dynamically balanced oxygen supply as determined by blood flow and arterial oxygen content and demand as determined by metabolism. Yet renal hemodynamics and oxygenation offer a number of striking differences vs. nonrenal tissues. Most organs extract approximately 45% of available oxygen (i.e., difference between arterial and venous blood) while the kidney only

Andreas Pohlmann and Thoralf Niendorf (eds.), *Preclinical MRI of the Kidney: Methods and Protocols*, Methods in Molecular Biology, vol. 2216, https://doi.org/10.1007/978-1-0716-0978-1_10,

extracts 10–15% of available oxygen. This is in part because, on a per gram basis, whole-kidney blood flow is higher than that of most other tissues. The kidneys while receiving 20–25% of cardiac output under resting conditions, only consume about 7% of the body's total oxygen. The major determinant of renal O_2 consumption is energy-dependent tubular sodium reabsorption. Whereas O_2 consumption determines perfusion in nonrenal tissues, renal O_2 consumption is largely determined by perfusion. Increased renal blood flow is, in general, accompanied by increased glomerular filtration rate, and therefore necessitates increased energy-dependent tubular sodium reabsorption. Another particularity is the highly heterogeneous blood perfusion and oxygenation within the kidney. Virtually all of the blood flowing into the kidney perfuses the cortex. The medulla is perfused by a small fraction (about 10% of total renal blood flow) of blood that had traversed the cortex. In accordance, tissue partial pressure of oxygen (pO_2) is very low in the medulla. Three additional mechanisms substantially contribute to low renal tissue pO_2. (a) The particular architecture of the intrarenal vasculature enables shunt diffusion of O_2 from arteries to veins in the cortex as well as from descending to ascending vasa recta in the medulla. (b) The vascular architecture also promotes differential distribution of erythrocytes and plasma at certain vessel branches (plasma skimming), which results in different hematocrit and O_2 content of blood perfusing the daughter vessels. (c) The Fåhræus–Lindqvist effect lowers the hematocrit in the long and narrow vasa recta supplying the medulla, which lowers the O_2 content of blood perfusing the medulla. At the same time, a rather high metabolic rate and thus O_2 demand is required to support active reabsorption of sodium along medullary thick ascending limbs of Henle's loop (mTAL) [1]. For a comprehensive description of the causes and the degree of the heterogeneity of intrarenal perfusion and oxygenation *see* the chapter by Cantow K et al. "Quantitative Assessment of Renal Perfusion and Oxygenation by Invasive Probes: Basic Concepts."

Given these particularities in renal oxygenation, there is an interest in understanding the physiological mechanisms involved in maintaining the oxygenation status within the medulla in health and how they may be affected in disease. Acute changes to intrarenal O_2 can be caused by both changes in O_2 supply due to changes in arterial O_2 content or perfusion, changes in O_2 consumption, or a combination of the two. For example, nitric oxide (NO) regulates blood supply by relaxing smooth muscle tension of resistance vessels and inhibitors of NO formation such as L-NAME reduce renal blood flow. The resulting reduction in renal O_2 supply decreases renal tissue oxygenation as evaluated by BOLD-MRI [2]. Alternatively, loop diuretics like furosemide block the sodium–potassium–chloride transporter in the mTAL. Inhibiting this secondary active transport decreases the load of the primary active sodium–

potassium pump (Na^+/K^+ ATPase) in the mTAL. The ensuing decrease in O_2-dependent sodium reabsorption results in an increase in outer medullary pO_2. Thus, administration of furosemide is most commonly used both as a validation of the measurements [3, 4] and as a tubular functional paradigm in the clinic [5]; for detailed discussion of the pros and cons *see* the chapter by Cantow K et al. "Reversible (Patho)Physiologically Relevant Test Interventions: Rationale and Examples." Early work using atrial natriuretic peptide (ANP), which was expected to cause some increase in blood flow, caused a significant decrease in both cortical and medullary O_2 due to the net increase in O_2 consumption related to sodium transport [6]. This illustrates the distinction between monitoring oxygenation vs. perfusion or blood flow and is especially relevant in the kidney.

In the setting of kidney disease, deregulation of O_2 balance has long been studied. A recent review [7] of gene responses in six different models of acute kidney injury (gram-negative sepsis, gram-positive sepsis, ischemia reperfusion, malignant hypertension, rhabdomyolysis, and cisplatin nephrotoxicity) found that hypoxia along with oxidative stress and inflammation was the common feature of all the disease models. These acute injuries may lead to tubule cell death by apoptosis or necrosis and injured cells frequently dedifferentiated into fibroblasts. This fibrosis can lead to tubular atrophy and reduction in function, forcing the remaining tubules to use more oxygen which can cause further injury [7].

Understanding the relationship between renal oxygenation and kidney disease was predominantly based on data obtained from preclinical models with tissue pO_2 measurements using invasive microprobes [3, 6, 8]. These probes were inserted in the kidney to provide local and acute pO_2 readings. Probe position is critical and can be difficult to maintain in small animals. Alternately, pimonidazole [9] can be used to stain tissue at severe hypoxia. This histological staining method only captures hypoxia present at the moment of tissue sampling. For detailed discussion of the advantages and disadvantages of these methods *see* the chapter by Cantow K et al. "Quantitative Assessment of Renal Perfusion and Oxygenation by Invasive Probes: Basic Concepts." BOLD MRI is a noninvasive imaging technique that can be used to estimate the relative oxygen availability in tissue. It offers both spatial information (at reduced spatial resolution compared to histology) and temporal resolution (typically lower than microprobes). Figure 1 illustrates the similarity and differences between histological, microprobe, and BOLD-MRI measurements. BOLD MRI allows for longitudinal follow-up because of its noninvasive nature.

In this chapter, we will provide an overview of BOLD MRI including the basic concept involved, and a few illustrative applications of renal BOLD MRI in rodents.

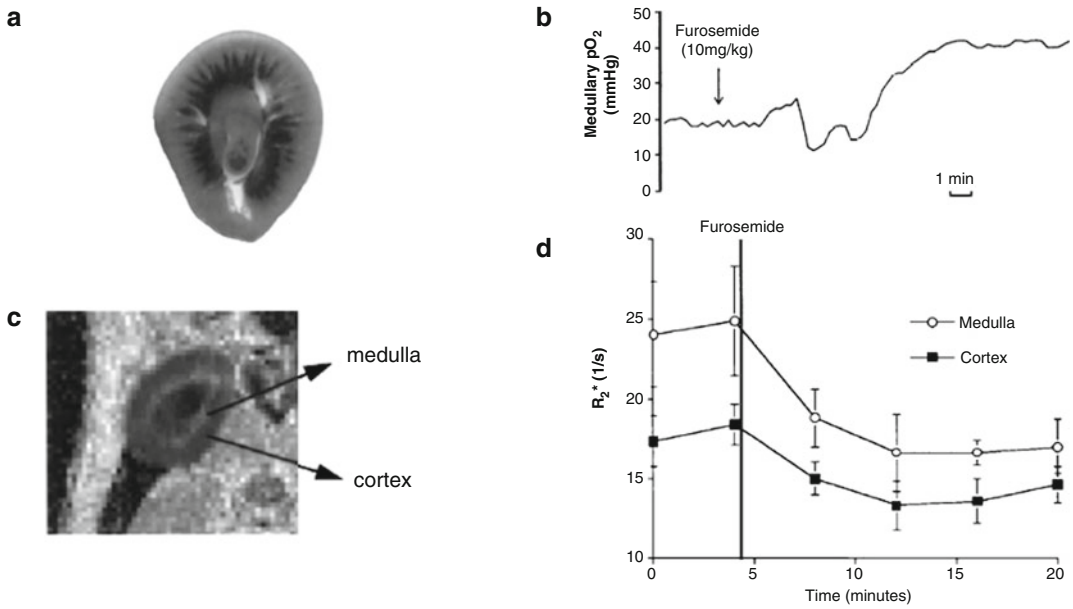

Fig. 1 (**a**) [10] A slice of rat kidney histologically stained for pimonidazole, showing the corticomedullary differences. Higher staining in the medulla is related to the increased hypoxia. This method can capture the spatial distribution of severe hypoxia within the kidney at the time of tissue sampling. (Reproduced from Zhong Z et al., *Am. J. Physiol.* 275 (*Renal Physiol.* 44): F595–F604, 1998 with permission from American Physiological Society). (**b**) [3] pO_2 microelectrode data showing the temporal changes in renal medullary pO_2 in a rat kidney and illustrates the increase in pO_2 following administration of furosemide. (Reproduced from Brezis M et al., *Am. J. Physiol.* 267 (*Renal Fluid Electrolyte Physiol.* 36): F1059–F1062, 1994 with permission from American Physiological Society). (**c**) [11] A representative slice of R_2* map in a rat kidney showing corticomedullary differences, even though the contrast is opposite compared to (**a**). The spatial resolution is also obviously lower compared to (**a**). (**d**) [11] Shows the changes in R_2* in the outer medulla and cortex after injection of furosemide. The first two points for both curves are baseline (preinjection). Both medullary and cortical R_2* drop after the injection of furosemide and stay relatively constant over the 20-min period of observation. Error bars represent standard deviation in the individual ROI measurements. This figure illustrates the merits of BOLD MRI in terms of providing both spatial and temporal information of pO_2 changes in kidneys. (Reproduced from Prasad PV et al., *J. Magn. Reson. Imaging* 1999; 9:842–846 with permission from John Wiley & Sons)

This introduction chapter is complemented by two separate chapters describing the experimental procedure and data analysis, which are part of this book.

This chapter is part of the book Pohlmann A, Niendorf T (eds) (2020) Preclinical MRI of the Kidney—Methods and Protocols. Springer, New York.

2 Measurement Concept

2.1 Basic Concept of BOLD Contrast

BOLD MRI technique uses deoxyhemoglobin (deoxyHb) as an intrinsic (or endogenous) contrast mechanism. Hemoglobin (Hb) is the primary vehicle for transporting O_2 in the blood. When O_2 is bound to Hb, it becomes oxyhemoglobin (oxyHb)

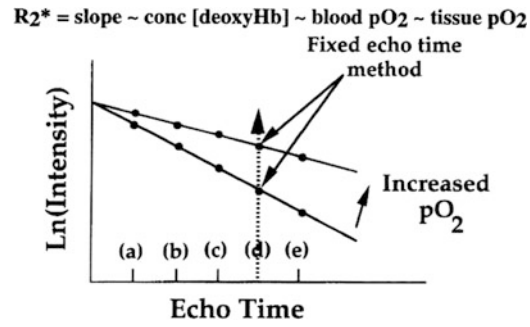

Fig. 2 [13]: Blood oxygenation level-dependent (BOLD) MRI changes qualitatively with pO_2. The deoxygenation of hemoglobin changes its magnetic characteristics, leading to changes in a parameter of magnetic resonance called R_2* (apparent spin–spin relaxation rate). R_2* can be estimated from signal intensity measurements made at several different echo times (**a**–**e**). The slope of Ln (intensity) vs. echo time determines R_2* and is directly related to the amount of deoxygenated blood. A decrease in the slope implies an increase in the pO_2 of blood. We can either measure the slope or obtain intensity measurements at a single echo time (e.g., **d**) to detect a difference in pO_2. Because blood pO_2 is thought to be in rapid equilibrium with tissue pO_2, changes in BOLD signal intensity or R_2* should reflect changes in the pO_2 of the tissue. (Reproduced from Prasad PV et al., Circulation. 1996 Dec 15; 94: 3271–5 with permission from American Heart Association)

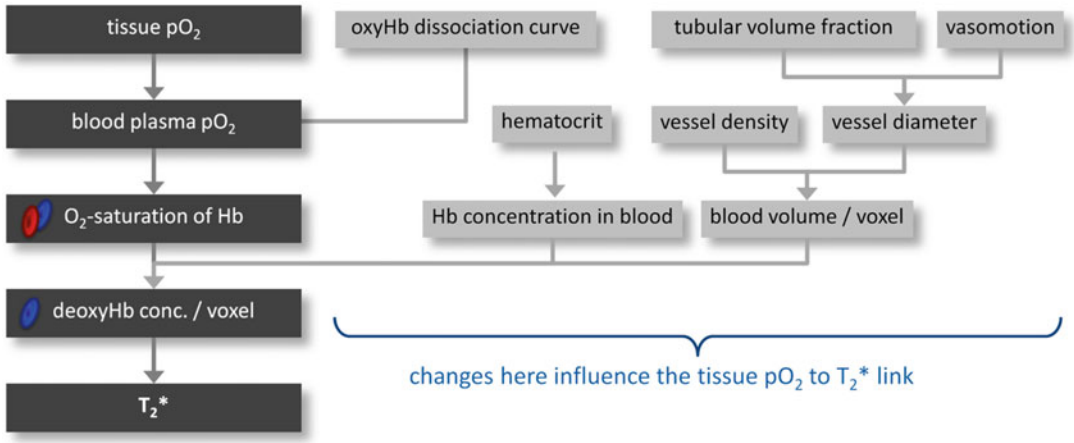

Fig. 3 [14]: Link between tissue pO_2 and T_2* (or R_2*), together with the potentially confounding factors

which is diamagnetic. When O_2 is released from Hb, it becomes deoxyhemoglobin (deoxyHb) which behaves as a paramagnet [12]. Since Hb is compartmentalized to the vascular system, the presence of deoxyHb creates local magnetic susceptibility gradients in and around blood vessels. This induces spin-dephasing so that the effective spin–spin relaxation decay of the MR signal governed by the relaxation time T_2* will be shortened when the local

deoxyHb concentration is increased. This results in signal loss in T_2*-weighted imaging (e.g., gradient echo (GRE) imaging) in areas of increased deoxyHb concentration. The BOLD signal is quantitatively measured by either the effective relaxation time T_2* (s) OR relaxation rate R_2* ($= 1/T_2$* and expressed in s^{-1}). T_2* and R_2* can be calculated based on GRE data acquired at different echo times (TE) and determining the slope of Ln (signal intensity) vs. TE (Fig. 2). With the assumption that hematocrit and local blood volume fraction remain unchanged (in fact, they might vary significantly), a decrease of R_2* corresponds to an increase of O_2 saturation of Hb and, assuming an unchanged oxyHb dissociation curve, in blood pO_2. Under "perfect" physiological conditions the pO_2 of capillary blood is thought to be in equilibrium with the surrounding tissue, and changes in observed R_2* could be interpreted as an indicator of changes in tissue pO_2. In many (patho)physiological scenarios however, the link between R_2* (T_2*), O_2 saturation of Hb, and tissue pO_2 is confounded by changes in various factors, which are illustrated in Fig. 3 and detailed in Subheading 2.3 [14].

The ratio of oxyHb to deoxyHb (which is the major determinant of % O_2 saturation of Hb under physiological conditions) is related to the pO_2 of blood and is governed by the oxyHb dissociation curve [15]. The renal medullary pO_2 is in the lower range of the curve. Hence a change in pO_2 will result in relatively larger change in the ratio of oxyHb to deoxyHb compared to a similar change in pO_2 of cortex. This makes BOLD MRI sensitive for following changes in pO_2 in the medulla.

2.2 BOLD MRI Acquisition Methods and Strategies for Kidney Oxygenation Measurement in Rodents

Two MR imaging techniques are used for renal BOLD MRI, namely, single shot echo planar imaging (EPI) [13] and multiple gradient echo (mGRE) sequences [4]. Functional imaging of the human brain predominantly uses single shot EPI due to the need for high temporal resolution and/or signal averaging. The ultrafast nature of EPI makes it ideal for abdominal imaging to freeze motion. It is suitable for applications with rapid changes in oxygenation and where R_2* mapping is not necessary [16]. However, it is highly sensitive to bulk magnetic susceptibility artifacts which results in image blurring, geometrical distortion, signal loss, and limited spatial resolution. The image distortion is amplified in regions with poor magnetic field homogeneity such as in the vicinity of bowels filled with gas. It is hardly used in preclinical setting, especially when using high field strength MR scanners.

mGRE sequence is currently the most widely utilized acquisition method both for human [4] and preclinical [11] applications of renal BOLD MRI. It acquires signals at multiple echo times after each excitation pulse. R_2* calculated as the slope of the straight line fitting of Ln(SI) vs. TE or by fitting the SI vs. TE data to a single decay monoexponential function. mGRE acquisitions provide improved SNR (signal-to-noise ratio), spatial resolution, and

image quality compared to single shot EPI method. However, longer echo times with mGRE sequence also suffer from bulk susceptibility artifacts. In preclinical setting, motion artifacts are usually minimized using multiple averages. mGRE can suffer from phase variations between odd and even echoes when both water and fat components are present in renal tissue. Choice of echo times corresponding to in-phase or out-of-phase can minimize such artifacts. In the presence of flow, use of even echoes may be preferred.

2.3 Limitations of BOLD MRI for Absolute pO_2 Measurement

R_2* inherently depends on many parameters, primarily including R_2 the natural spin–spin relaxation rate and a susceptibility weighted component termed R_2' ($R_2^* = R_2 + R_2'$). R_2' is determined by the susceptibility component. In the context of BOLD MRI, it depends on the amount of deoxyHb present within the voxel which is determined by the combination of fractional blood volume (fraction of the voxel occupied by blood), hematocrit, and O_2 saturation of hemoglobin.

The factors confounding the relationship between R_2^*(or T_2^*) and intrarenal blood pO_2 are listed in Table 1.

BOLD MRI is inherently best suited to monitor changes in regional pO_2 which is assumed to be in a dynamic equilibrium with O_2 saturation of Hb. This inherently assumes that there are no concomitant changes in fractional blood volume, the oxyHb dissociation curve, and hematocrit. While this may be valid with certain pharmacological maneuvers, one or more of these confounders will change in various acute scenarios. Any vasodilation or vasoconstriction, either induced by pharmacologic maneuvers or by endogenous control of renal vessels, alters the blood volume fraction. Besides the vasculature, the interstitial and the tubular compartments can also experience rapid volume changes and, given the rather rigid renal capsule, can therefore modulate the blood volume fraction. The tubular volume fraction is a unique feature of the kidney; it is quite large and can rapidly change due to (a) changes in glomerular filtration, (b) alterations in tubular outflow toward the pelvis, (c) modulation of the transmural pressure gradient, and (d) changes in resorption. This is partly the motivation to establish R_2^* vs. tissue pO_2 calibration relationship. However, such calibration is strictly valid only in the model it was established in, for example, healthy animals and cannot be generalized to disease models and other species including humans. Mathematical analytical methods can be used to model the relationship between R_2' and O_2 saturation of Hb [17, 18]. However, these will require knowledge of fractional blood volume and regional hematocrit for the individual kidney. In kidneys, it is known that hematocrit is lower in the inner medulla [19]. This explains why inner medulla in rodents usually have low R_2^* values (typically lower than the cortex and erroneously indicating more availability of oxygen). Fractional blood volume is inherently an imaging specific concept and so

Table 1
Factors confounding the relationship between R_2*(or T_2*), oxygen saturation of hemoglobin, and blood pO_2

Confounding factor	Direction of effect	Examples scenarios
Blood volume fraction	Positive	Vasodilation/constriction, change in tubular volume fraction
Hematocrit	Positive	Plasma skimming, hemodilution
Oxygen–hemoglobin dissociation curve		Changes in pH, pCO_2, or temperature
Magnetic field (B_0) inhomogeneity	Positive	Bowel gas, poor shim
T_2	Positive	Edema

A "positive" direction of the effect means that an increase in the confounding factor leads to an increase in R_2* (decrease in T_2*) and hence an overestimation of the hypoxia

there is very little literature on its measurement. The ideal method to estimate fractional blood volume is by using an intravascular contrast agent such as ultrasmall paramagnetic iron oxide (USPIO) [20, 21]. Oxygen saturation of Hb is related to the pO_2 of blood by the oxyHb dissociation curve which is influenced by factors such as pH, pCO_2, and temperature. Further the inherent assumption that blood pO_2 is in a dynamic equilibrium with surrounding tissue pO_2 may not hold in disease [22]. These limitations of BOLD MRI need to be taken in to account when interpreting experimental findings as illustrated recently [14]. In order to study the detailed link between renal tissue pO_2 and T_2* in vivo, an integrated approach that combines parametric MRI and quantitative physiological measurements (MR-PHYSIOL) was proposed [23]. The MR-PHYSIOL setup was used to study the relationship between renal T_2* and tissue pO_2 and perfusion in rats. The findings indicate that changes in T_2* qualitatively reflect changes in renal tissue pO_2 induced by maneuvers including hyperoxia, suprarenal aortic occlusion, and hypoxia. Yet a closer examination of the quantitative relationships between relative changes in T_2* and in tissue pO_2 revealed discrepancies, indicating that, due to the differential changes in one or more of the confounders, simple translation of quantitative results obtained for one intervention of renal hemodynamics and oxygenation to another intervention is falling short of being appropriate. Also, taking the perfusion and oxygenation heterogeneity among the kidney layer into account, extrapolation of results obtained for one layer to others must be made with due caution [24].

2.3.1 R_2' Measurement

Given the specific interest in the susceptibility component of spin–spin relaxation rate for BOLD MRI, measurement of R_2' is desired. While there has been some effort in directly estimating R_2' using

asymmetric spin-echo sequences [25], a simpler and practical method may be to perform a gradient echo and spin echo measurement to estimate R_2* and R_2 separately then calculate the difference [26]. Since R_2 can independently vary with certain pharmacological maneuvers (e.g., following L-NAME [21]), using R_2' as the BOLD MRI parameter may be more specific to the oxygenation related changes. A recent study illustrated the feasibility of using R_2' measurements to estimate blood oxygenation in rat kidneys [17]. While R_2 is not directly sensitive to BOLD effects, there is actually an indirect dependence due to diffusion effects of spins experiencing the field gradients generated by the presence of deoxyHb in the microvasculature. In this regard, R_2 has been shown to be more specific to small vessels [27], while R_2* is typically weighted by larger vessels.

2.4 Considerations Regarding Animal Preparation

- Bowel gas can create susceptibility artifacts in renal R_2* map, right lateral position helps minimize susceptibility artifacts from bowel gas.
- Respiratory motion could create artifacts and usually multiple measurements for averaging purposes can be used to minimize these. Alternately, respiratory triggering could be used but may increase the acquisition times.
- Studies indicate the choice of anesthesia has a large influence on renal R_2* [28]. This may be partly due to known effects of anesthesia on respiration, temperature, blood pressure, and hence pO_2.

3 Overview of Preclinical Applications

Noninvasive BOLD MRI is primarily attractive for the use in humans. However, there is a need for preclinical applications of the method primarily to validate the technique against invasive measures and better understand changes in different diseases.

Validation of renal BOLD MRI measurements is mostly carried out by comparing the responses to certain (patho)physiologically relevant test interventions or pharmacological maneuvers against pO_2 measurements using invasive microprobes [2, 29]. BOLD data was compared with pimonidazole staining in 10-week-old mice [30]. Interestingly, pimonidazole staining did not show differences between db/db and db/m mice, even though BOLD MRI showed significant differences (Fig. 4). This is probably related to the fact that pimonidazole detects severe hypoxia, typically $pO_2 < 10$ mmHg. There was one study in swine where the invasive probe was placed in the contralateral kidney compared to the one where BOLD MRI measurements were made [31]. This study

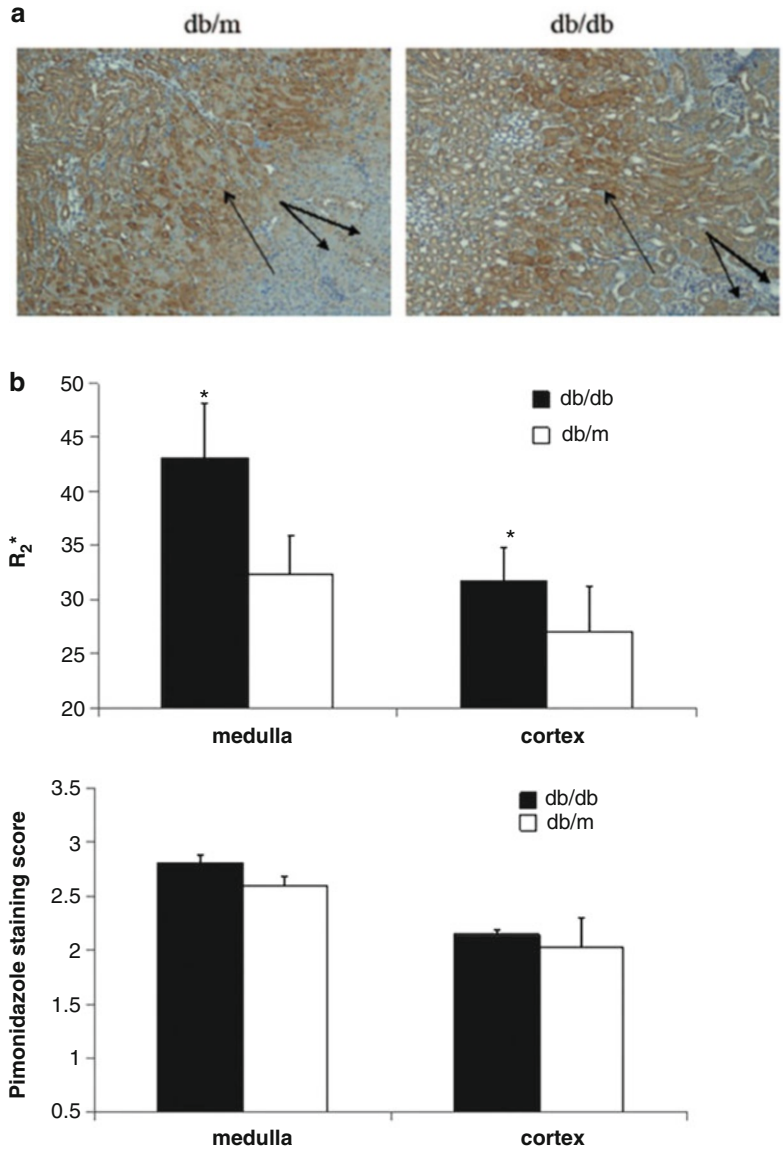

Fig. 4 [30]: (**a**) Pimonidazole immunohistochemical staining of the kidney of db/m and db/db mouse (magnification 100×). Strong pimonidazole (brown) staining of renal tubules was observed mainly in the outer medulla (single arrows) both from db/m and db/db mouse. Weaker staining was seen in the cortex of both db/db and db/m mice (double arrows). (**b**) A summary of R_2* values obtained by BOLD MRI in the medulla and cortex of 10-week-old db/db and db/m mice (upper panel). R_2* is higher in medulla than cortex in both db/db and db/m reflecting lower oxygenation in the medulla. The asterisk denotes a significant difference in R_2* between db/db and db/m in both cortex ($P < 0.04$) and medulla ($P < 0.001$). The lower panel shows the pimonidazole staining score for db/db and db/m mice of similar age (10 weeks old). The medulla had stronger staining than the cortex in both db/db and db/m reflecting increased hypoxia. No significant differences were found in the pimonidazole staining of the medulla and cortex between db/db and the db/m mice. The lack of significance with pimonidazole may be partly related to the fact that it is only sensitive to severe hypoxia, that is, $pO_2 < 10$ mmHg. (Reproduced from Prasad PV et al., Invest Radiol 2010; 45: 819–822 with permission from Wolters Kluwers Health Inc.)

proposed the use of R_2* vs. pO_2 as a calibration curve for translating BOLD MRI measurements in to pO_2 estimates. More recently, true simultaneous measurements with both BOLD MRI and invasive probes were demonstrated in rats [23]. Interventions such as hypoxia, hyperoxia, and suprarenal aortic occlusion were studied by use of this MR-PHYSIOL setup [24]. Use of high field small animal scanners is ideal for rodent applications in terms of signal-to-noise ratios. However, renal BOLD MRI can also be effectively conducted in rats using whole body scanners at both 1.5 [11] and 3 T [32] routinely used in humans which have more widespread availability. Renal BOLD MRI in mice has been shown to be feasible at 3 T using a custom surface radiofrequency loop coil for signal reception [30, 33].

Early application of renal BOLD MRI was primarily to evaluate acute effects of physiological or pharmacological maneuvers. Administration of furosemide increased medullary oxygenation predominantly due to reduction in O_2 consumption [3, 6]. Given the role of NO in essential hypertension, we have also observed differential response to administration of L-NAME in healthy rats compared to spontaneously hypertensive rats (SHR) [34]. Because the reduced NO availability in SHR is related to oxidative stress, we also observed a differential response to free radical scavenger (tempol) in SHR rats compared to controls [35].

3.1 Application to Disease Models

Acute kidney injury (AKI) is a sudden episode of kidney failure or kidney damage that happens within a few hours or a few days of an insult such as administration of nephrotoxins. AKI is common in patients who are hospitalized, patients who have underlying kidney disease, and especially in older adults. Medullary hypoxic injury plays a major role in the pathogenesis of AKI [7], as has been studied by both invasive probes and BOLD MRI in rat models of X-ray contrast induced AKI and renal ischemia/reperfusion injury [36–38].

Given the role of endothelial dysfunction in the susceptibility to contrast induced AKI, we have studied the additive effects of L-NAME, indomethacin (prostaglandin inhibitor) followed by iodinated radio-contrast medium iothalamate (Fig. 5) [32]. Using this AKI model, we compared the effects of different contrast media based on different physicochemical properties, observed large increases in R_2* in the inner-stripe of outer medulla [39]. In a similar model, we evaluated potential preventative maneuvers such as preadministration of furosemide or N-acetylcysteine (NAC, an antioxidant). We found that furosemide was effective in abolishing the increase in R_2* post-radiocontrast [40]. These observations matched with a decrease in urinary neutrophil gelatinase associated lipocalin (NGAL) measurements, a marker of tubular injury.

Unilateral ureteral obstruction (UUO) is a commonly used model of renal fibrosis [41]. However, permanent ligation of ureter

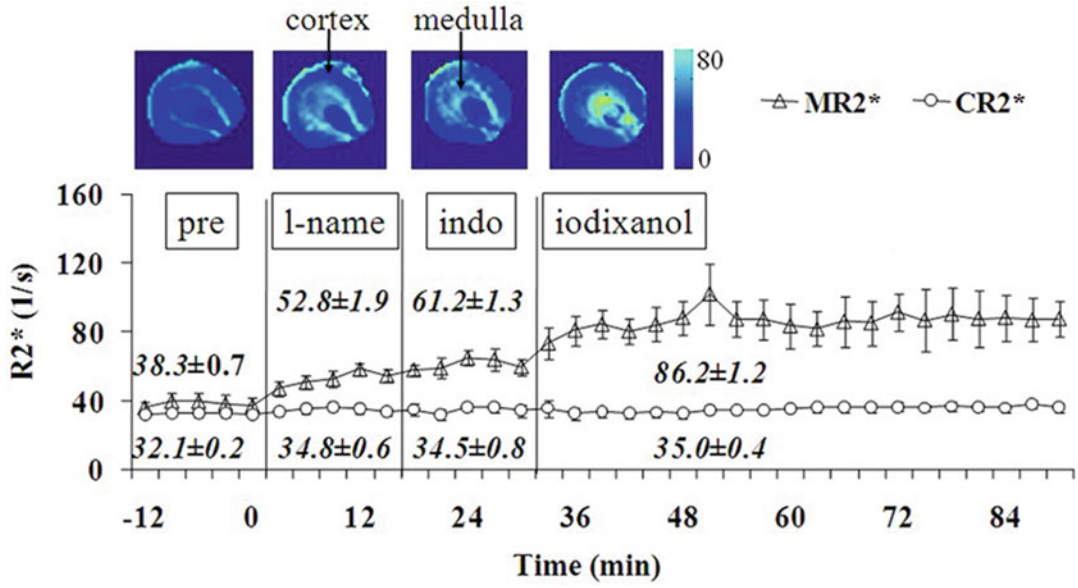

Fig. 5 [32]: Averaged (mean ± SE) renal R_2* time course from six rats in renal medulla and cortex following the administration of L-NAME, indomethacin, and radio-contrast iodixanol. The vertical lines indicate the time of administration of each of chemicals. Pre: baseline; l-name: L-NAME; indo: indomethacin. Error bars represent standard error among rats. On the top are R_2* maps generated using custom Matlab (Mathworks, Natick, MA, USA) code in one representative rat. The relative brightness in renal outer medulla suggests low oxygenation level compared to cortex. The window settings were the same in all maps. The brightness in renal outer medulla increases gradually after each chemical, suggesting the progressively decreasing of oxygenation. The R_2* maps are from baseline, following administration of L-NAME, indomethacin, and iodixanol. The arrows show the renal outer medulla and cortex where the ROIs were placed. The renal outer medulla is relatively brighter than renal cortex in baseline R_2* map, suggesting lower oxygenation level there. Each chemical contributes to the additional increased brightness in R_2* maps in the renal outer medulla, suggesting progressive hypoxia in the renal outer medulla. Bottom: shows the corresponding plot of R_2* vs. time. (Reproduced from Prasad PV et al., J. Magn. Reson. Imaging 2012; 36:1162–1167 with permission from John Wiley & Sons)

results in complete loss of renal parenchyma within couple of weeks. A reversible unilateral ureteral obstruction (rUUO) was proposed as a more representative model of chronic kidney disease (CKD) [42]. In rUUO model, the microvascular clip used to ligate the ureter is moved distally every 2 days for 6 days and then removed. BOLD MRI was used to monitor the longitudinal changes at 2 and 28 days following reversal of the UUO [43]. This application is an illustration of the advantage of a noninvasive imaging method in performing longitudinal studies within the same animal.

Acknowledgments

Work supported, in part, by grant funding from the National Institutes of Health (R01 DK093793 and R01 DK106557).
This publication is based upon work from COST Action PARENCHIMA, supported by European Cooperation in Science and Technology (COST). COST (www.cost.eu) is a funding agency for research and innovation networks. COST Actions help connect research initiatives across Europe and enable scientists to enrich their ideas by sharing them with their peers. This boosts their research, career, and innovation.
PARENCHIMA (renalmri.org) is a community-driven Action in the COST program of the European Union, which unites more than 200 experts in renal MRI from 30 countries with the aim to improve the reproducibility and standardization of renal MRI biomarkers.

References

1. Brezis M, Rosen S (1995) Hypoxia of the renal medulla--its implications for disease. N Engl J Med 332(10):647–655. https://doi.org/10.1056/NEJM199503093321006
2. Li LP, Ji L, Santos EA, Dunkle E, Pierchala L, Prasad P (2009) Effect of nitric oxide synthase inhibition on intrarenal oxygenation as evaluated by blood oxygenation level-dependent magnetic resonance imaging. Investig Radiol 44(2):67–73. https://doi.org/10.1097/RLI.0b013e3181900975
3. Brezis M, Agmon Y, Epstein FH (1994) Determinants of intrarenal oxygenation. I. Effects of diuretics. Am J Physiol 267(6 Pt 2): F1059–F1062
4. Prasad PV, Chen Q, Goldfarb JW, Epstein FH, Edelman RR (1997) Breath-hold R2* mapping with a multiple gradient-recalled echo sequence: application to the evaluation of intrarenal oxygenation. J Magn Reson Imaging 7(6):1163–1165
5. Prasad PV, Li LP, Thacker JM, Li W, Hack B, Kohn O, Sprague SM (2019) Cortical perfusion and tubular function as evaluated by magnetic resonance imaging correlates with annual loss in renal function in moderate chronic kidney disease. Am J Nephrol 49(2):114–124. https://doi.org/10.1159/000496161
6. Brezis M, Heyman SN, Epstein FH (1994) Determinants of intrarenal oxygenation. II. Hemodynamic effects. Am J Physiol 267 (6 Pt 2):F1063–F1068
7. Hultstrom M, Becirovic-Agic M, Jonsson S (2018) Comparison of acute kidney injury of different etiology reveals in-common mechanisms of tissue damage. Physiol Genomics 50 (3):127–141. https://doi.org/10.1152/physiolgenomics.00037.2017
8. Aukland K, Krog J (1960) Renal oxygen tension. Nature 188:671. https://doi.org/10.1038/188671a0
9. Rosenberger C, Rosen S, Paliege A, Heyman SN (2009) Pimonidazole adduct immunohistochemistry in the rat kidney: detection of tissue hypoxia. Methods Mol Biol 466:161–174. https://doi.org/10.1007/978-1-59745-352-3_12
10. Zhong Z, Arteel GE, Connor HD, Yin M, Frankenberg MV, Stachlewitz RF, Raleigh JA, Mason RP, Thurman RG (1998) Cyclosporin A increases hypoxia and free radical production in rat kidneys: prevention by dietary glycine. Am J Phys 275(4):F595–F604. https://doi.org/10.1152/ajprenal.1998.275.4.F595
11. Priatna A, Epstein FH, Spokes K, Prasad PV (1999) Evaluation of changes in intrarenal oxygenation in rats using multiple gradient-recalled echo (mGRE) sequence. J Magn Reson Imaging 9(6):842–846
12. Buxton RB (2013) The physics of functional magnetic resonance imaging (fMRI). Rep Prog Phys 76(9):096601. https://doi.org/10.1088/0034-4885/76/9/096601
13. Prasad PV, Edelman RR, Epstein FH (1996) Noninvasive evaluation of intrarenal oxygenation with BOLD MRI. Circulation 94 (12):3271–3275. https://doi.org/10.1161/01.cir.94.12.3271

14. Niendorf T, Pohlmann A, Arakelyan K, Flemming B, Cantow K, Hentschel J, Grosenick D, Ladwig M, Reimann H, Klix S, Waiczies S, Seeliger E (2015) How bold is blood oxygenation level-dependent (BOLD) magnetic resonance imaging of the kidney? Opportunities, challenges and future directions. Acta Physiol 213(1):19–38. https://doi.org/10.1111/apha.12393
15. Severinghaus JW (1979) Simple, accurate equations for human blood O2 dissociation computations. J Appl Physiol Respir Environ Exerc Physiol 46(3):599–602. https://doi.org/10.1152/jappl.1979.46.3.599
16. Schachinger H, Klarhofer M, Linder L, Drewe J, Scheffler K (2006) Angiotensin II decreases the renal MRI blood oxygenation level-dependent signal. Hypertension 47 (6):1062–1066. https://doi.org/10.1161/01.HYP.0000220109.98142.a3
17. Thacker J, Zhang JL, Franklin T, Prasad P (2017) BOLD quantified renal pO2 is sensitive to pharmacological challenges in rats. Magn Reson Med 78(1):297–302. https://doi.org/10.1002/mrm.26367
18. Zhang JL, Morrell G, Rusinek H, Warner L, Vivier PH, Cheung AK, Lerman LO, Lee VS (2014) Measurement of renal tissue oxygenation with blood oxygen level-dependent MRI and oxygen transit modeling. Am J Physiol Renal Physiol 306(6):F579–F587. https://doi.org/10.1152/ajprenal.00575.2013
19. Zimmerhackl B, Robertson CR, Jamison RL (1985) The microcirculation of the renal medulla. Circ Res 57(5):657–667
20. Pohlmann A, Cantow K, Huelnhagen T, Grosenick D, Dos Santos PJ, Boehmert L, Gladytz T, Waiczies S, Flemming B, Seeliger E, Niendorf T (2017) Experimental MRI monitoring of renal blood volume fraction variations en route to renal magnetic resonance oximetry. Tomography 3(4):188–200. https://doi.org/10.18383/j.tom.2017.00012
21. Storey P, Ji L, Li LP, Prasad PV (2011) Sensitivity of USPIO-enhanced R2 imaging to dynamic blood volume changes in the rat kidney. J Magn Reson Imaging 33(5):1091–1099. https://doi.org/10.1002/jmri.22526
22. Evans RG, Leong CL, Anderson WP, O'Connor PM (2007) Don't be so BOLD: potential limitations in the use of BOLD MRI for studies of renal oxygenation. Kidney Int 71 (12):1327–1328; author reply 1328. https://doi.org/10.1038/sj.ki.5002321
23. Cantow K, Arakelyan K, Seeliger E, Niendorf T, Pohlmann A (2016) Assessment of renal hemodynamics and oxygenation by simultaneous magnetic resonance imaging (MRI) and quantitative invasive physiological measurements. Methods Mol Biol 1397:129–154. https://doi.org/10.1007/978-1-4939-3353-2_11
24. Pohlmann A, Arakelyan K, Hentschel J, Cantow K, Flemming B, Ladwig M, Waiczies S, Seeliger E, Niendorf T (2014) Detailing the relation between renal T2* and renal tissue pO2 using an integrated approach of parametric magnetic resonance imaging and invasive physiological measurements. Investig Radiol 49(8):547–560. https://doi.org/10.1097/RLI.0000000000000054
25. Zhang X, Zhang Y, Yang X, Wang X, An H, Zhang J, Fang J (2013) Feasibility of noninvasive quantitative measurements of intrarenal R (2)' in humans using an asymmetric spin echo echo planar imaging sequence. NMR Biomed 26(1):91–97. https://doi.org/10.1002/nbm.2823
26. Yang X, Cao J, Wang X, Li X, Xu Y, Jiang X (2008) Evaluation of renal oxygenation in rat by using R2' at 3-T magnetic resonance: initial observation. Acad Radiol 15(7):912–918. https://doi.org/10.1016/j.acra.2008.01.015
27. Boxerman JL, Hamberg LM, Rosen BR, Weisskoff RM (1995) MR contrast due to intravascular magnetic susceptibility perturbations. Magn Reson Med 34(4):555–566
28. Niles DJ, Gordon JW, Fain SB (2015) Effect of anesthesia on renal R2 * measured by blood oxygen level-dependent MRI. NMR Biomed 28(7):811–817. https://doi.org/10.1002/nbm.3314
29. dos Santos EA, Li LP, Ji L, Prasad PV (2007) Early changes with diabetes in renal medullary hemodynamics as evaluated by fiberoptic probes and BOLD magnetic resonance imaging. Investig Radiol 42(3):157–162. https://doi.org/10.1097/01.rli.0000252492.96709.36
30. Prasad P, Li LP, Halter S, Cabray J, Ye M, Batlle D (2010) Evaluation of renal hypoxia in diabetic mice by BOLD MRI. Invest Radiol 45 (12):819–822. https://doi.org/10.1097/RLI.0b013e3181ec9b02
31. Pedersen M, Dissing TH, Morkenborg J, Stodkilde-Jorgensen H, Hansen LH, Pedersen LB, Grenier N, Frokiaer J (2005) Validation of quantitative BOLD MRI measurements in kidney: application to unilateral ureteral obstruction. Kidney Int 67(6):2305–2312. https://doi.org/10.1111/j.1523-1755.2005.00334.x
32. Li LP, Franklin T, Du H, Papadopoulou-Rosenzweig M, Carbray J, Solomon R, Prasad PV (2012) Intrarenal oxygenation by blood

oxygenation level-dependent MRI in contrast nephropathy model: effect of the viscosity and dose. J Magn Reson Imaging 36 (5):1162–1167. https://doi.org/10.1002/jmri.23747

33. Li LP, Ji L, Lindsay S, Prasad PV (2007) Evaluation of intrarenal oxygenation in mice by BOLD MRI on a 3.0T human whole-body scanner. J Magn Reson Imaging 25 (3):635–638. https://doi.org/10.1002/jmri.20841
34. Li L, Storey P, Kim D, Li W, Prasad P (2003) Kidneys in hypertensive rats show reduced response to nitric oxide synthase inhibition as evaluated by BOLD MRI. J Magn Reson Imaging 17(6):671–675. https://doi.org/10.1002/jmri.10301
35. Li LP, Li BS, Storey P, Fogelson L, Li W, Prasad P (2005) Effect of free radical scavenger (tempol) on intrarenal oxygenation in hypertensive rats as evaluated by BOLD MRI. J Magn Reson Imaging 21(3):245–248. https://doi.org/10.1002/jmri.20260
36. Hoff U, Lukitsch I, Chaykovska L, Ladwig M, Arnold C, Manthati VL, Fuller TF, Schneider W, Gollasch M, Muller DN, Flemming B, Seeliger E, Luft FC, Falck JR, Dragun D, Schunck WH (2011) Inhibition of 20-HETE synthesis and action protects the kidney from ischemia/reperfusion injury. Kidney Int 79(1):57–65. https://doi.org/10.1038/ki.2010.377
37. Arakelyan K, Cantow K, Hentschel J, Flemming B, Pohlmann A, Ladwig M, Niendorf T, Seeliger E (2013) Early effects of an x-ray contrast medium on renal T2 */T2 MRI as compared to short-term hyperoxia, hypoxia and aortic occlusion in rats. Acta Physiol 208(2):202–213. https://doi.org/10.1111/apha.12094
38. Seeliger E, Flemming B, Wronski T, Ladwig M, Arakelyan K, Godes M, Mockel M, Persson PB (2007) Viscosity of contrast media perturbs renal hemodynamics. J Am Soc Nephrol 18 (11):2912–2920. https://doi.org/10.1681/ASN.2006111216
39. Li LP, Lu J, Zhou Y, Papadopoulou MV, Franklin T, Bokhary U, Solomon R, Sen A, Prasad PV (2014) Evaluation of intrarenal oxygenation in iodinated contrast-induced acute kidney injury-susceptible rats by blood oxygen level-dependent magnetic resonance imaging. Invest Radiol 49:403–410. https://doi.org/10.1097/RLI.0000000000000031
40. Li LP, Thacker J, Lu J, Franklin T, Zhou Y, Papadopoulou MV, Solomon R, Prasad PV (2014) Efficacy of preventive interventions for iodinated contrast-induced acute kidney injury evaluated by intrarenal oxygenation as an early marker. Invest Radiol 49(10):647–652. https://doi.org/10.1097/RLI.0000000000000065
41. Togao O, Doi S, Kuro-o M, Masaki T, Yorioka N, Takahashi M (2010) Assessment of renal fibrosis with diffusion-weighted MR imaging: study with murine model of unilateral ureteral obstruction. Radiology 255 (3):772–780. https://doi.org/10.1148/radiol.10091735
42. Puri TS, Shakaib MI, Chang A, Mathew L, Olayinka O, Minto AW, Sarav M, Hack BK, Quigg RJ (2010) Chronic kidney disease induced in mice by reversible unilateral ureteral obstruction is dependent on genetic background. Am J Physiol Renal Physiol 298(4): F1024–F1032. https://doi.org/10.1152/ajprenal.00384.2009
43. Haque ME, Franklin T, Bokhary U, Mathew L, Hack BK, Chang A, Puri TS, Prasad PV (2014) Longitudinal changes in MRI markers in a reversible unilateral ureteral obstruction mouse model: preliminary experience. J Magn Reson Imaging 39(4):835–841. https://doi.org/10.1002/jmri.24235